

# Influence of Residual Stresses on Corrosion and Wear Behavior of Electrodeposited Nanocrystalline Cobalt-Phosphorus Coatings

Nayef M. Alanazi, A.M. El-Sherik, Saleh H. Alamar and Shouwen Shen

Research & Development Center, Saudi Aramco, Saudi Arabia, Box 62, Dhahran 31311

\*E-mail: [nayef.anazi@aramco.com](mailto:nayef.anazi@aramco.com)

Received: 15 May 2013 / Accepted: 29 June 2013 / Published: 1 August 2013

---

Electrodeposited nanocrystalline Cobalt-Phosphorus (Co-P) alloy coatings deposited onto carbon steel substrates at different phosphorous contents (0.0 wt%, 3 wt% and 10 wt%) were investigated for the influence of residual stress on their corrosion and wear behaviors. X-ray diffraction technique was employed to determine the average crystallite size and residual stresses. The electrochemical corrosion behavior of Co-P coatings compared with a pure nanocrystalline cobalt coating was investigated using open circuit potential and potentiodynamic polarization scans. Wear resistance of electrodeposited nanocrystalline Co-P coatings was tested using pin-on-disc tribometer. The experimental results showed that with increasing phosphorous content, the average crystallite size decreased and coating compressive residual stresses increased. Also, the experimental results revealed that wear and corrosion resistance of Co-P coatings initially increased with increasing compressive residual stress of coating reaching a maximum at residual stresses of 450 MPa and 500 MPa before dropping with further increase in the compressive residual stress.

---

**Keywords:** Nanocrystalline cobalt-phosphorus coatings, residual stress, corrosion behavior and wear resistance.

## 1. INTRODUCTION

Electrodeposited nanocrystalline Cobalt-Phosphorus (Co-P) coatings have been the subject of intensive research [1-3] for replacement of the environmentally unfriendly hard chrome coatings in tribological applications. Nanocrystalline Co-P coatings showed ultrahigh strength, improved superplastic extensibility [4], and superior wear resistance [5] as compared with their conventional counterparts. Moreover, these coatings have been also shown to possess good magnetic properties, i.e., high saturation magnetization [6] and good thermal stability [7]. Previous investigations have indicated

that the addition of phosphorus led to better resistance to aqueous corrosion [8] for crystalline and amorphous alloys. There are studies reported on corrosion behavior of electrodeposited Co-P coatings [9-12]. Several research works indicated that low phosphorous Co-P ( $\geq 3$  wt%) coatings are crystalline and the high phosphorous Co-P (5-15 wt%) coatings are amorphous. It was found also that the amorphous alloyed coatings protect the substrate more effectively than the crystalline alloyed coatings [13, 14]. V. Ezhil et al., [12] studied thoroughly the electrochemical corrosion behavior of pulse and DC electrodeposited Co-P coatings. The electrochemical results revealed that the overall corrosion rate was lower for the pulse deposited coatings than the DC deposited coating. High phosphorous Co-P coatings exhibited an amorphous structure, which in turn improved the corrosion resistance because of their grain size reduction and the passive film formed on their surfaces.

Although, effect of residual stress on the corrosion and wear resistance of electrodeposited nanocrystalline Co-P coatings were not studied. In the current study, the corrosion behavior of electrodeposited nanocrystalline Co-P coatings was examined in 3.5% NaCl solution using open circuit potential and potentiodynamic polarization techniques and compared with electrodeposited nanocrystalline Co. Wear resistance of electrodeposited nanocrystalline Co-P coatings using pin-on-disc tribometer was also conducted. The objective of this work is to study the effect of residual stress on corrosion and wear behavior of electrodeposited nanocrystalline Co-P coatings.

## 2. EXPERIMENTAL PROCEDURE

Nanocrystalline Co and Co-P alloy coatings were prepared by the electrodeposition process using developed procedures described elsewhere [15, 16]. Nanocrystalline Co-P samples were electrodeposited from a bath containing cobalt sulfate, boric acid, sodium chloride (NaCl) and saccharine onto flat 45 mm x 45 mm carbon steel (AISI 1010) to an average thickness of 250  $\mu\text{m}$ . The amount of phosphorus co-deposited with cobalt was controlled by the phosphoric concentration in the plating bath. The bulk concentration of phosphorus in nanocrystalline Co-P was 3 wt% and 10 wt% and this is referred to as Co3P and Co10P, respectively. Environmental scanning electron microscope (SEM) was used to observe the nanocrystalline Co and Co-P alloy coatings morphology after corrosion tests. The crystallite size and the residual stresses of the prepared Co-P coatings were examined by X-ray diffraction (XRD) technique utilizing a PANalytical X'Pert PRO instrument operated at 45 kV and 40 mA with Cu  $\alpha$  radiation ( $\lambda = 1.5418 \text{ \AA}$ ). A  $0.01^\circ$  step size and 2 second per step were used for crystallite size determination in the range of  $10^\circ$  to  $160^\circ$   $2\theta$  scan. A  $0.02^\circ$  step size and 20 second per step were set for residual stress analysis in the range of  $44^\circ$  to  $47^\circ$   $2\theta$  of multiple scans at different tilt angles ( $\psi$ ) of  $0^\circ$ ,  $21.41^\circ$ ,  $31.08^\circ$ ,  $39.22^\circ$ ,  $46.90^\circ$ ,  $54.72^\circ$ ,  $63.42^\circ$  and  $75^\circ$ . The corrosion behavior was studied by means of open circuit potential and potentiodynamic polarization scans. The test electrode was immersed in deaerated 3.56 wt% NaCl solution; and a standard circular ( $1.00 \text{ cm}^2$ ) area of specimen was exposed to the solution at room temperature. The electrochemical measurements were performed using a conventional three-electrode cell, where the nanocrystalline Co and Co-P alloy coatings were the test electrodes, with a saturated calomel electrode (SCE) as a reference electrode, and platinum as the counter electrode. Prior to starting the potentiodynamic polarization scans, the test

electrode was allowed to stabilize for approximately 60 min. Immediately following the stabilization period, the test electrode was polarized at a scan rate of 1.66 mV/s from an initial potential of  $-1$  V (vs. OCP) to the final potential of  $+1$  V. The corrosion potential ( $E_{corr}$ ), corrosion current density ( $I_{corr}$ ) and anodic/cathodic Tafel slopes ( $\beta_A$  and  $\beta_C$ ) were calculated from these tests using the proprietary CorrWare® software compiled and marketed by Scribner Associates Inc. Then, based on the approximate linear polarization at the corrosion potential ( $E_{corr}$ ), polarization resistance ( $R_p$ ) values were determined using the relationship [17]:

$$R_p = \frac{\beta_A \times \beta_B}{2.3 \times i_{corr} \times (\beta_A + \beta_B)} \quad (1)$$

Non-perforating dry sliding wear was conducted on developed coatings using a pin-on-disc tribometer where the test sample slides against a stationary alumina ball with a diameter of 6 mm at room temperature. The ball is pressed by 7 N load on the test samples, which rotate with a linear velocity of 0.15 ms<sup>-1</sup>, 4 mm of wear scare radius and sliding distance 1,000 m.

### 3. RESULTS AND DISCUSSION

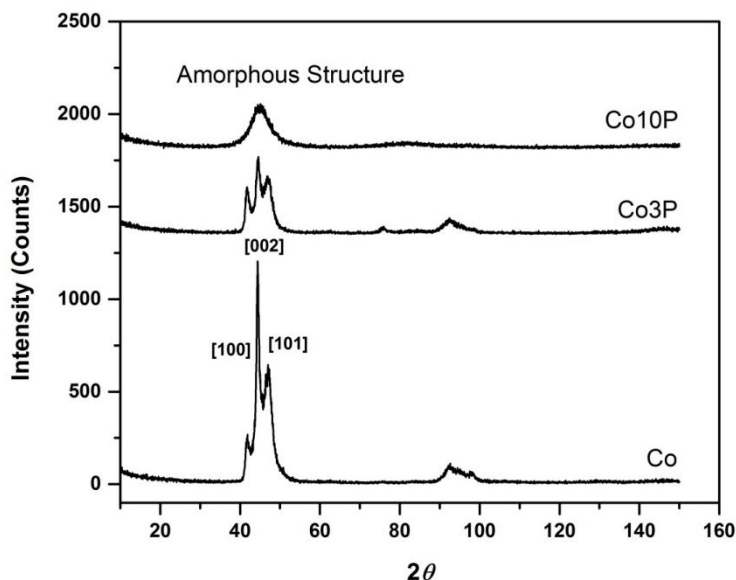
#### 3.1. Residual stress and crystal size

Figure 1 shows the XRD pattern of electrodeposited nanocrystalline Co and Co-P coatings. It can be seen clearly that the intensity of peaks decreased with increasing the phosphorus content showing a considerable peak broadening due to the ultra-fine grain size. In addition, the average crystal size of the nanocrystalline Co and Co-P coatings was calculated from XRD patterns using Scherrer's equation, Eq. 2, [18] given by:

$$Dv = k\lambda / \beta \cos\theta \quad (2)$$

The results of residual stress and crystallite size calculated from the diffraction peak of Co-P (002) at  $44.5^\circ$  ( $2\theta$ ) for nanocrystalline Co and Co-P coatings are shown in Figure 2. The results showed that the crystal size decreased with increasing the phosphorus content of the Co coatings. The crystal size of the nanocrystalline Co-P coating with phosphorus content of 3 wt% reduced to 8 nm compared to that obtained from pure nanocrystalline Co coating, which was 21 nm. When the phosphorus content in Co coating was increased to 10 wt%, amorphous structure was formed.

In the present study, the  $\sin^2\psi$  analysis method [19] was used to measure residual stress of nanocrystalline Co and Co-P coatings. The d-spacing was plotted against  $\sin^2\psi$  for each sample. The calculation of the residual stresses was automatically performed by the software of X'Pert Stress using the slopes "m,"  $\sigma = \frac{mE}{d_0(1+\nu)}$ . The negative values indicate compressive stress whereas the positive values indicate tensile stress. The results of residual stress showed that all samples exhibited compressive stresses (negative, from 200 MPa to 647 MPa). With increasing the phosphorous content, the compressive residual stresses in coatings increased. Compressive stresses in coatings are known to improve adhesion between deposits and substrate and to prevent from the development of fatigue cracks [20].



**Figure 1.** XRD pattern of nanocrystalline Co, Co3P and Co10P coatings.

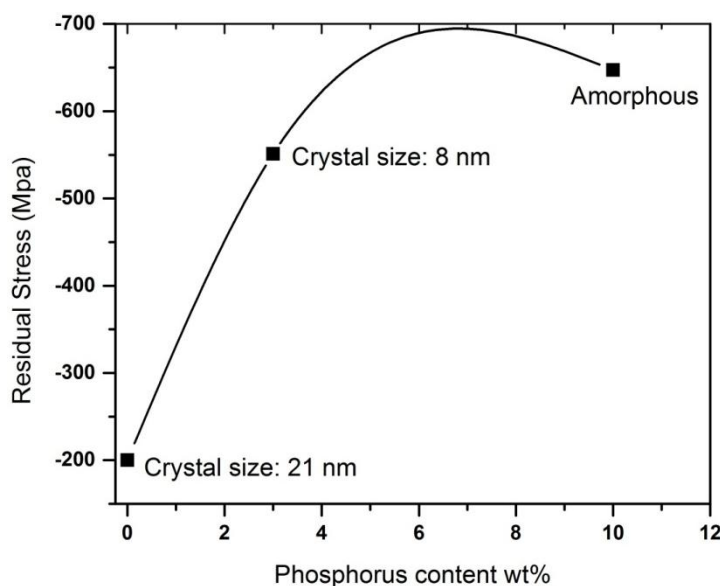


**Figure 2.** Residual stress and crystallite size of nanocrystalline Co, Co3P and Co10P coatings.

### 3.2. Open Circuit Potential (OCP)

The open circuit potential vs. immersion time of all coated samples was recorded and plotted as shown in Figure 3. Pure nanocrystalline Co coating initially exhibited a potential of  $-0.46$  V (vs. SCE) in NaCl solution. The potential then increased slightly, in the first five minutes of immersion, to reach  $-0.43$  V. This is attributed to the formation of oxide film on the coating surface. Then, the potential dropped sharply to reach  $-0.56$  V, which is close to the potential value of Co3P. This indicated that sharp decrease in potential is a result of breakdown film, which may be formed during sample preparation before starting the OCP test. The potentials of Co3P and Co10P were found to be stable

during the OCP test, -0.56 V and -0.49 V, respectively. The potential of Co10P was found to be nobler value ( $\approx 70$  mV) than that of Co3P. The significantly nobler potential value of Co10P can be interpreted to the positive effect of the P alloying on the corrosion resistance of the Co coating.

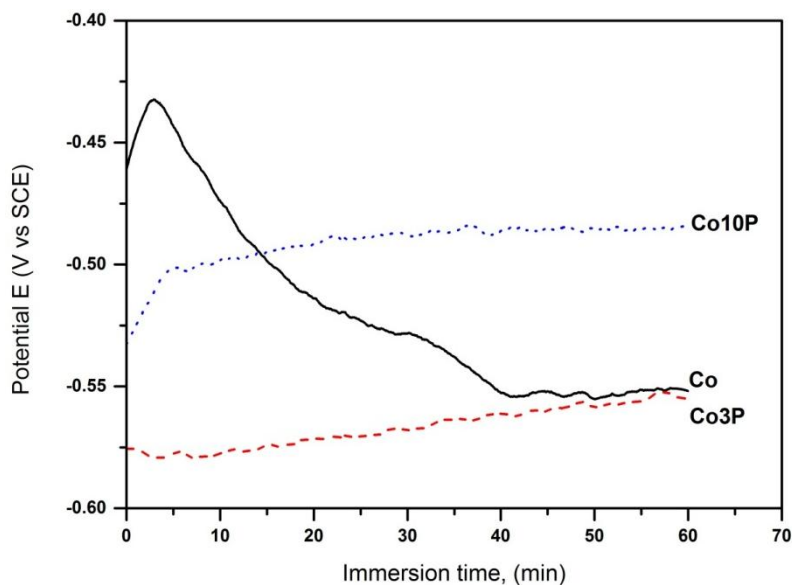


**Figure 3.** Open circuit potential vs. immersion time for nanocrystalline Co, Co3P and Co10P coatings.

### 3.3. Potentiodynamic polarization scan

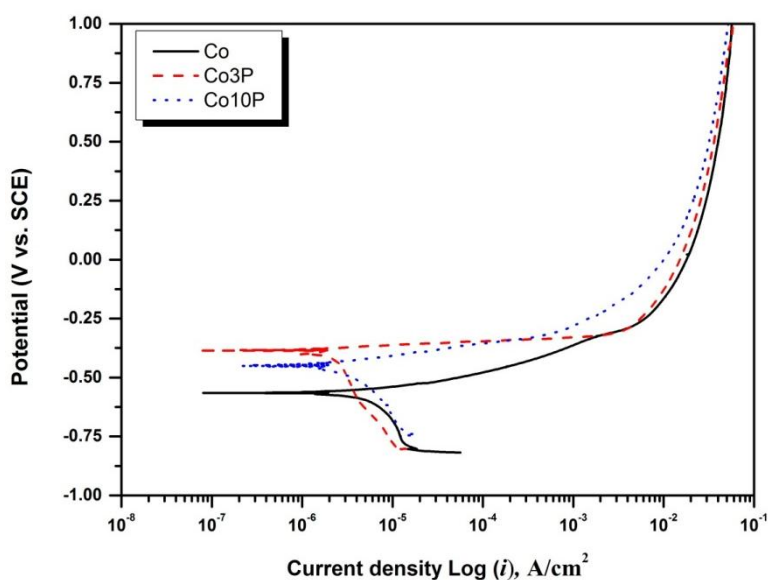


**Figure 4.** Polarization curves of electrodeposited nanocrystalline Co, Co 3wt% P and Co10 wt% P coatings immersed in 3.56% NaCl solution.

The corrosion behavior of the Co-P coatings was evaluated through the potentiodynamic polarization technique and the polarization curves are shown in Figure 4. These data show that the

corrosion resistance of nanocrystalline Co and Co-P coatings is substantially different. Upon increasing the anodic polarization, all samples displayed active behavior without any distinctive transition to passivation up to the resulting current density of  $1 \text{ mA/cm}^2$ . The corrosion potential of the alloyed coatings shifted towards more positive compared to the nanocrystalline Co coating, indicating an improved corrosion resistance of the coatings. Co3P showed better corrosion resistance than Co10P, where the corrosion potential of the nanocrystalline Co coating increased by 169 mV and 107 mV after alloying with 3 wt% and 10 wt% phosphorous, respectively. Figure 5 shows phosphorous content vs. corrosion rate. It can be seen that that an increase in phosphorous content in the Co coating decreased the corrosion rate of the coating with the lowest corrosion rate reached at approximately 3 wt% Co. Further increase in the P content increased the corrosion rate.

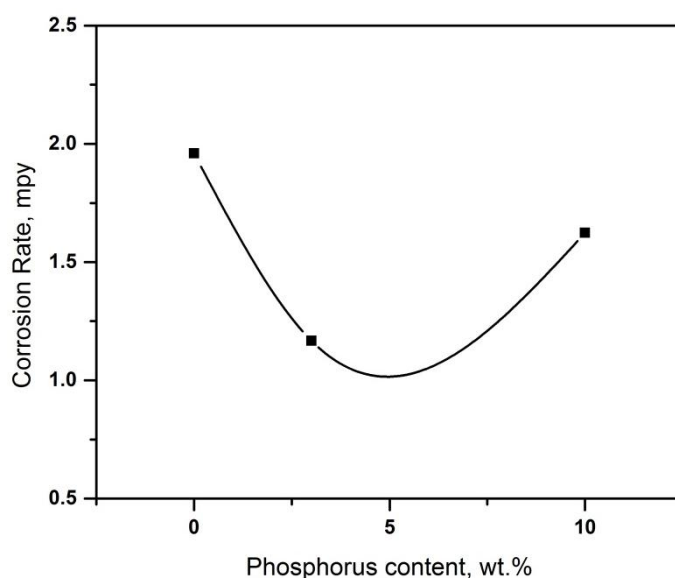


**Figure 5.** Effect of phosphorus content on corrosion performance of coating.

Figure 6 shows SEM images of the corroded surface of Co, Co3P and Co10P coatings after potentiodynamic polarization scans in 3.56% NaCl solution. Nanocrystalline Co and Co3P coatings showed uniform corrosion with no appearance of cracks or pits. In contrast, Co10P exhibited severe corrosion attack and large cracks were observed on the surface. Observed large cracks are the result of high compressive residual stresses on Co10P coating.

It was reported [13, 14] that amorphous structure provides good corrosion protection in 3.5% NaCl solution for alloyed coating with phosphorus compared to crystalline structure. In this work, however, the coating with amorphous structure exhibited lower corrosion resistance, which can be explained to the negative influence of residual stresses on coating corrosion barrier protection. Figure 7 shows the effect of coating residual stress on electrochemical results obtained from potentiodynamic polarization scans. It can be seen clearly that increasing coating compressive residual stresses to 500 MPa increased coating corrosion potential and decreased corrosion current. When the coating compressive residual stress value exceeded 500 MPa, the coating corrosion potential decreased sharply

and increased in corrosion current. These results are in agreement with SEM analysis on the corroded surface as shown in Figure 6c, where microcracks, like dry mud, were observed.

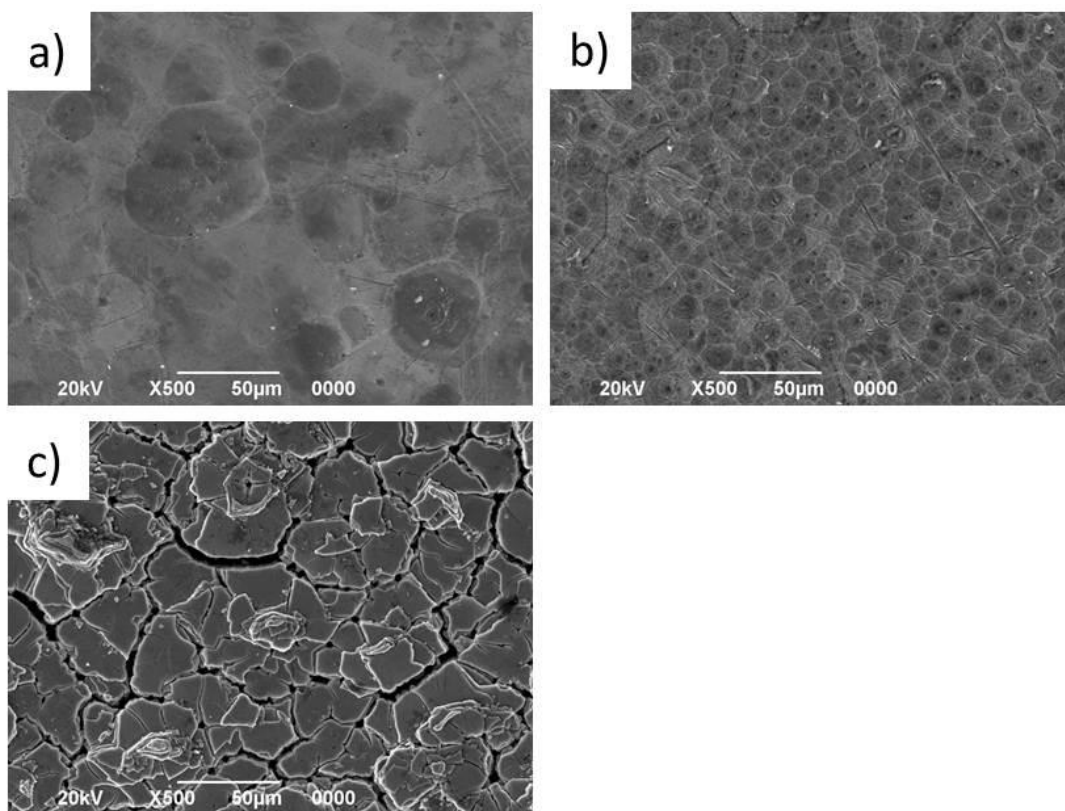


**Figure 6.** SEM images of corroded surfaces after exposure to potentiodynamic tests; (a) Co, (b) Co3P and (c) Co10P.

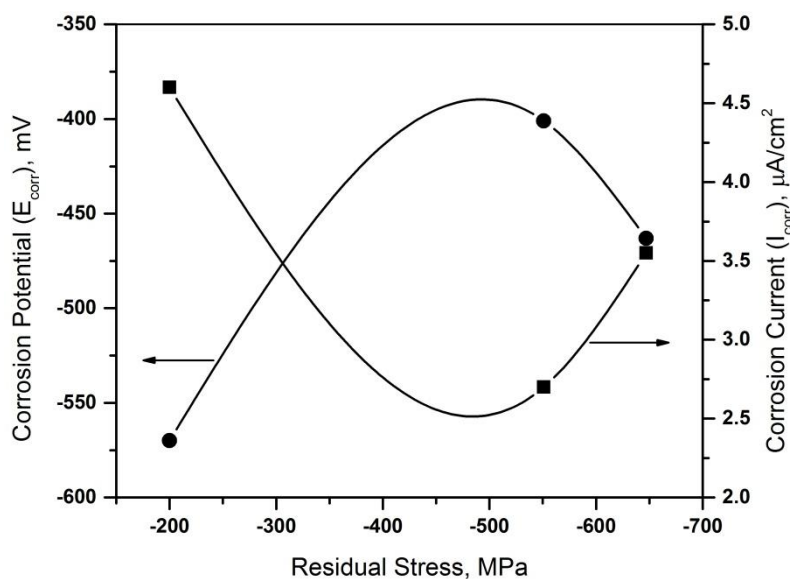


**Figure 7.** Corrosion potential and corrosion current vs. residual stresses.

### 3.4. Wear resistance

The specific wear rate was measured using volume loss as measured by mass loss. The weight of the samples was measured to the nearest 0.01 mg before and after the wear test to determine mass loss. According to Archard [21], the wear volume is proportional to both force and the distance and the wear resistance can be defined as the inverse of wear rate ( $\text{Nm}/\text{mm}^3$ ). The specific wear rate can be calculated by Eq. 3:

$$k = \frac{V}{FS} \quad \& \quad V (\text{mm}^3) = \frac{\text{mass loss, g}}{\text{density, g/cm}^3} \times 1000 \quad (3)$$

Figure 8 shows the effect of residual stress on the wear resistance of the nanocrystalline Co and Co-P coatings. The results revealed that the wear resistance of nanocrystalline Co and Co-P coatings does not increase linearly with increasing the residual stress. It can be seen clearly that the Co3P coating showed the best wear resistance. The increase compressive residual stress of Co-P coatings of more than -450 MPa degraded the wear resistance of coating. The Co10P coating, which is the highest compressive residual stress (-647 MPa), exhibited lower wear resistance compared to other coatings.

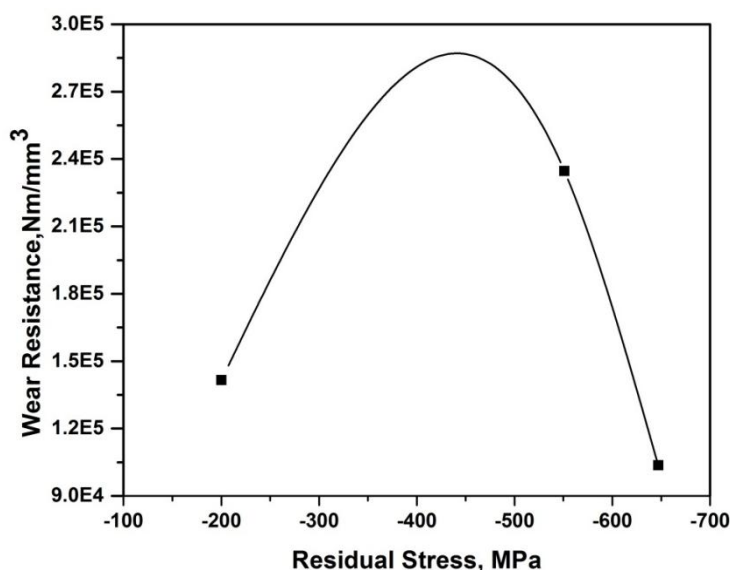


**Figure 8.** Effect of residual stress on the wear resistance of nanocrystalline Co and Co-P coatings.

## 4. CONCLUSION

Nanocrystalline Co and Co-P coatings were electroplated onto carbon steel substrate from sulfate bath at different phosphorus weight percentages. The results showed that the Co3P coating is the best corrosion and wear resistance. Increase phosphorus content of Co-P coatings to 10 wt% would degrade their corrosion barrier and wear protections. Residual stress measurements revealed that alloying nanocrystalline Co coating with phosphorous increases the compressive residual stress of the coatings. The intuitive correlations between residual stresses of nanocrystalline Co-P coatings and their wear and corrosion resistance were not observed. It was noticed that wear and corrosion resistance of

coating increased with increased compressive residual stress of coating until it reached 450 MPa to 500 MPa. Further increase in the compressive residual stresses reduced both wear and corrosion resistance. These results were also confirmed with the SEM studies carried out on the corroded samples.

#### ACKNOWLEDGMENTS

The authors would like to acknowledge Saudi Aramco for giving permission to publish the results. Also, they acknowledge the Research & Development Center for financial support and technical help in this research.

#### References

1. K.S. Kumar, H. Van Swygenhoven and S. Suresh, *Acta Mater.*, 51 (2003) 5743.
2. L. Lu, Y.F. Shen, X.H. Chen, L.H. Qian and K. Lu, *Science*, 304 (2004) 422.
3. L. Lu, M.L. Sui and K. Lu, *Science*, 287 (2000) 1463.
4. A.A. Karimpoor, U. Erb, K.T. Aust, Z. Wang and G. Palumbo, *Material Sci. Forum*, 386-388 (2002) 415.
5. J. McCrea, G. Palumbo, F. Gonzalez, A. Roberson and K. Ponagiotopoulos, proceedings of the AESF SUR/FIN: 2001, American Electroplaters and Surface Finishers Society, 2001, p. 138.
6. M.J. Aus, C. Cheung, B. Szpunar and U. Erb, *J. Mater. Sci. Lett.*, 17 (1998) 1949.
7. G. Hibbard, K.T. Aust, G. Palumbo and U. Erb, *Scr. Mater.*, 44 (2001), 513.
8. M.A. Helfand, C.R. Clayton, R.B. Diegel and N.R. Sorenson, *J. Electrochem. Soc.*, 139 (8) (1992) 2121.
9. H. Jung and A. Alfantazi, *Corrosion*, 63 (No. 2) (2007) 159.
10. H. Jung and A. Alfantazi, *Electrochim. Acta*, 51 (2006) 1806.
11. A. Aledresse and A. Alfantazi, *J. Material Science*, 39 (2004) 1523.
12. V. Ezhil Slvi, H. Seenivasan and K.S. Rajam, *Surface & Coating Technology*, 206 (2012) 2199-2206.
13. T.S.N. SankaraNarayanan, I. Baskaran, K. Krishnaveni and S. Parthiban, *Surface & Coating Technology*, 200 (2006) 3438.
14. H. Ashassi-Sorkhabi and S.H. Rafizadeh, *Surface & Coating Technology*, 176 (2004) 318.
15. U. Erb and A.M. El-Sherik, U.S. Patent No. 5,353,266, October 1994.
16. U. Erb, A.M. El-Sherik, C. Cheung and M.J. Aus, U.S. Patent No. 5,433,797, July 1995.
17. D.W. Shoesmith, ASM Metals Corrosion Handbook, Vol. 13, 1987, p. 49.
18. Patterson, A., "The Scherrer Formula for X-Ray Particle Size Determination", *Phys. Rev.* 56 (10): 978-982
19. M.E. Hilley, Residual Stress Measurement by X-Ray Diffraction, SAE J784a, Society of Automotive Engineers, New York, 1971, 21-24.
20. A.A. Solov'ev, N.S. Sochugov and K.V. Oskomov, *The Phys. of Mate. and Metallo.*, 109 (2) (2010) 111.
21. J.F. Archard, *Tribol. Int.*, 9 (1976), 242-243.